Collision-Free Workspace Design Optimisation of the 3-DOF Gantry-Tau Parallel Kinematic Machine

Ilya Tyapin
The University of Queensland
Brisbane, Australia
Email: ilya@itee.uq.edu.au

Abstract

One of the main advantages of the Gantry-Tau machine is a large accessible workspace/footprint ratio compared to many other parallel machines. The Gantry-Tau improves this ratio by allowing a change of assembly mode without internal link collisions or collisions between the links and the moving *TCP* platform. This paper introduces an optimisation scheme based on the geometric approach for the workspace area and the functional dependencies of the elements of the static matrix and the minimum distance between two links to define the collisions between robot's links. The results show that by careful design of the manipulated platform, a collision free workspace can be archived. Kinematic design obtained by optimisation according to this paper gives a workspace/footprint ratio of more than 3.5. In addition, a workspace optimisation method is presented where the parameters are the support frame lengths and the robot's arm lengths.

1 Introduction

The Tau family of PKMs was invented by ABB Robotics, see Brogårdh (2002). The Gantry-Tau was designed to overcome the workspace limitations while retaining many advantages of PKMs such as low moving mass, high stiffness and no link twisting or bending moments. For a given Cartesian position of the robot each arm has two solutions for the inverse kinematics, referred to as the left- and right-handed configurations. While operating the Gantry-Tau in both left- and right-handed configurations, the workspace will be significantly larger in comparison with both a serial Gantry-type robot and other PKMs with the same footprint and with only axial forces in the links of the arms. The intended application of the robot is for machining operations requiring a workspace equal to or larger than of a typical serial-type robot, but with higher stiffness. However, the robot can also be designed for very fast material handling and assembly or for high precision processes such as laser cutting, water jet cutting and measurement.

In this paper the triangular-link variant of the 3-DOF Gantry-Tau structure is considered, which was first presented in Brogårdh, Hanssen and Hovland (2005). Triangular mounted links give several advantages: they enable a reconfiguration of the robot and a larger reach is obtained in the extremes of the workspace. When using parallel links, the orientation of the manipulated platform will be constant, which increases the risk of collisions of the arms with the manipulated platform in the extremes of the workspace area.

In Johannesson, Berbyuk and Brogårdh (2004) a basic workspace optimisation method for the 3-DOF Gantry-Tau with no triangular links was presented. Two geometrical parameters of the machine were optimised to maximise the cross-sectional workspace area. Our paper is an extension of the work in Johannesson, Berbyuk and Brogårdh (2004). The new contributions of this paper are: the optimisation is made for the Gantry-Tau with triangular mounted links, the optimisation is made over the whole workspace volume and not just the cross-sectional workspace area, the detection of the collisions between links is added to the optimisation. The geometric approach for the Gantry-Tau reachable workspace area calculation was presented in Tyapin, Hovland and Brogårdh (2007) for the first time.

Using geometrical methods the workspace can be calculated as an intersection of simple geometrical objects, Merlet (2000), for example spheres. Design optimisation was attempted by Chablat and Wenger (2003), Liu, Wang and Gao (2000) and Monsarrat and Gosselin (2003). In addition, Liu, Wang and Gao (2000) presented the relationships between the workspace and link lengths of all planar 3-DOF parallel manipulator. In Monsarrat and Gosselin (2003) the workspace was defined by three rotational angles. In our paper the static matrix was presented by one platform rotational angle α.

Another interesting work is the paper by Kim, Chung and Youm (1997). In that paper a fully geometric approach to calculate the reachable workspace was presented for a 6-DOF Hexapod type PKM. The differences compared to our paper are the use of variable link lengths instead of fixed actuators at the robot base and no design optimisation was attempted in Kim, Chung and Youm (1997). The closest work to this paper was presented in Bonev and Ryu (2001) for the orientation workspace, but both Kim, Chung and Youm (1997) and Bonev and Ryu (2001) use the inverse kinematics (rotational matrix) to define the workspace.

The distance between two geometric objects (lines, segments of lines, rays, surfaces etc.) is defined as the minimum distance between two points on these objects.

The closest works to the method shown in section 3 were presented in Eberly (2001) and Teller (2008), but both use a vector cross products to define the closest distance between two line segments in 3D plane. In addition, in Eberly (2001) partitioning of the *st*-plane by the unit square is used, but the unit square searching algorithm has more cases and is more complicated to be implemented. Another interesting work was presented in Murray, Hovland and Brogård (2006). The method in Murray, Hovland and Brogård (2006) is based on the method proposed by Hudgens and Arai (1993) and involves calculating the minimum perpendicular distance between two finite line segments. In Murray, Hovland and Brogård (2006) and Hudgens and Arai (1993) vector cross products are also used but the collisions free workspace of 5-DOF the Gantry-Tau was found first. Also, no functional analysis of the distance function in 2D plane is attempted in both Eberly (2001) and Teller (2008).

The main benefit of the work in this paper is the savings in computational effort. As a result, the method presented in this paper is more accurate and faster. The time saving is possible because the conditional equations will be found from a functional dependency.

Brief descriptions of the kinematics is presented in sections 2. In section 3 the general information about a distance between two line segments is presented. The conditional equations and collisions analysis is presented in section 4. The combined optimisation problem is formulated in section 5. The results are shown in section 6 and finally the conclusions are presented in section 7.

2 Kinematic Description

In this section the kinematic description of the 3-DOF Gantry-Tau parallel kinematic machine is presented. The kinematics of the basic Gantry-Tau structure has been described earlier in Johannesson, Berbyuk and Brogårdh (2004). The difference in the current 3-DOF version of the Gantry-Tau compared to the basic version analysed in Johannesson, Berbyuk and Brogårdh (2004) is that two of the links in the three-link arm are mounted in a triangular constellation instead of in parallel. The triangular-link version of the Gantry-Tau kinematic model is illustrated in Fig.1. The 3-

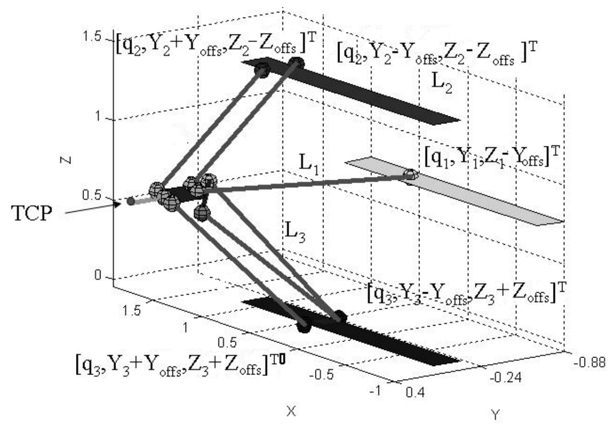

Figure 1: *Triangular-link variant of the Gantry-Tau shown in the left-handed configuration for all link clusters.*

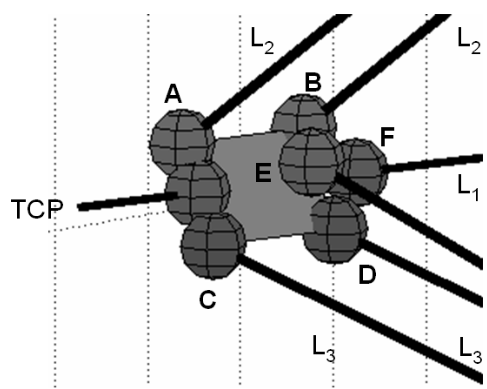

Figure 2: *Kinematic platform parameters.*

DOF Gantry-Tau can be manually reconfigured while the 5-DOF version, see Hovland, Choux, Murray, Tyapin and Brogårdh (2008), can be automatically reconfigured while avoiding singularities. As for the basic Gantry-Tau structure, each of the 3 parallel arms (lengths L_1, L_2 and L_3) is controlled by a linear actuator with actuation variables q_1, q_2 and q_3. The actuators in Fig. 1 are aligned in the direction of the global X coordinate. The arm connected to actuator q_1 consists of one single link. The arm connected to actuator q_2 consists of two parallel links. The arm connected to actuator q_3 consists of three links, where two links are mounted as a triangle. The link lengths and actuator positions are constant.

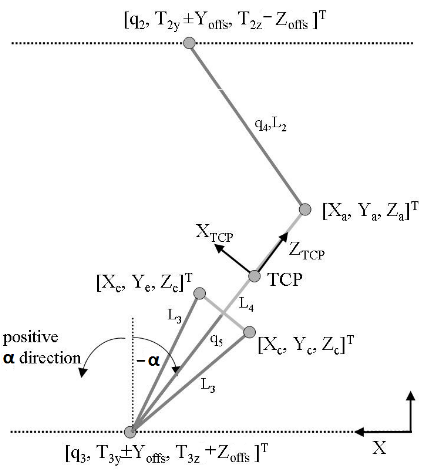

Figure 3: *Kinematic parameters in XZ-plane.*

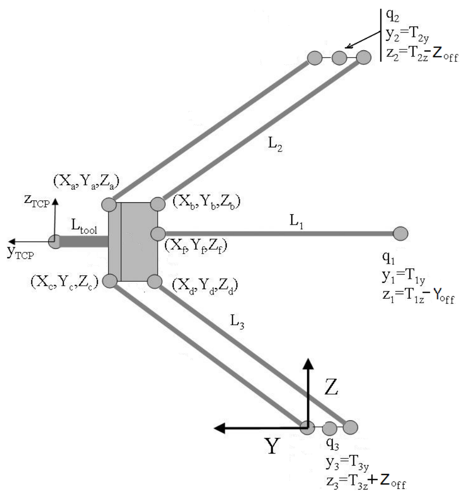

Figure 4: *Kinematic parameters in YZ-plane.*

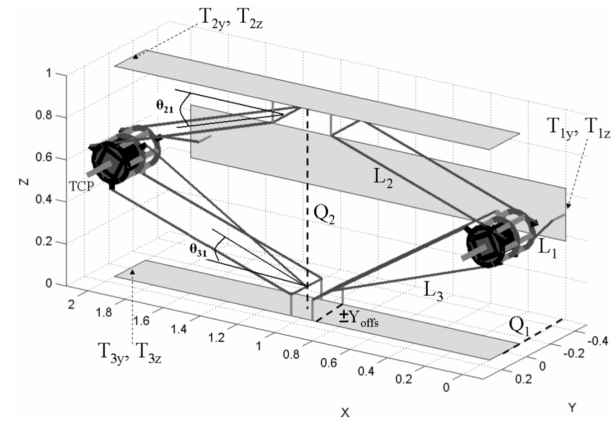

Figure 5: *The 3-DOF reconfigurable Gantry-Tau robot.*

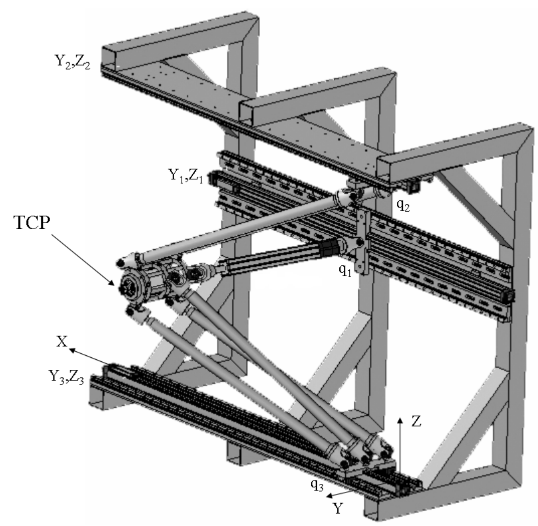

Figure 6: *A prototype of the 3-DOF Gantry-Tau with a triangular-mounted link pair.*

Fig. 2 shows the manipulated platform. The points A, B, C, D, E and F are the link connection points. The arm with one single link connects the actuator q_1 with platform point F. The arm with two links connects actuator q_2 with the platform points A and B. The arm with three links connects actuator q_3 with the platform points C, D and E. Fig. 3 shows a projection of the link system in Fig. 1 into the XZ-plane and Fig. 4 a projection into the YZ-plane.

Fig. 5 shows the PKM structure in both the left-handed and right-handed configuration (also called assembly or working modes). The Tau structure is characterised by a clustering of the links in groups of 1, 2 and 3, respectively, with fixed link lengths L_1, L_2 and L_3. Three linear actuators are used at the base to move the three arms independently in the global X direction. More details about the inverse and forward kinematics of the Gantry-Tau can be found in Brogårdh, Hanssen and Hovland (2005) and Williams, Hovland and Brogårdh (2006).

The actuator track locations are fixed in the Y and Z directions and the locations are denoted T_{1y}, T_{1z}, T_{2y}, T_{2z}, T_{3y} and T_{3z}, respectively (see Figs.4, 5 and 1). The dimensioning of the PKM's support frame is given by the two variables Q_1 and Q_2 as illustrated in Fig. 5, where Q_1 is the depth and Q_2 is the height. The width of the machine in the X direction is given by the length of the actuators.

For 5-DOF the Gantry-Tau with the triangular link pair the platform points $A-F$ are rotated in the following order: First a rotation of $r_y = \alpha$ about the platform Y axis which initially coincides with the global Y axis. Second a rotation r_z about the global Z axis and third a rotation r_x about the global X axis. The angle rotation α is performed first to avoid an additional transformation from the platform Y -axis to the global Y -axis. The platform points $A-F$ in the TCP coordinate frame are calculated as follows.

$$\begin{aligned}
[a_x\ a_y\ a_z]^T &= R_y(0)\ [0\ (-L_{tool})\ (R_p + L_{pin} + \frac{L_b}{2})]^T \\
[b_x\ b_y\ b_z]^T &= R_y(0)\ [0\ (-L_{tool} - L_p)\ (R_p + L_{pin} + \frac{L_b}{2})]^T \\
[c_x\ c_y\ c_z]^T &= R_y\ (\frac{2\pi}{3})\ [0\ (-L_{tool})\ (R_p + L_{pin} + \frac{L_b}{2})]^T \\
[d_x\ d_y\ d_z]^T &= [c_x\ b_y\ c_z]^T \\
[e_x\ e_y\ e_z]^T &= R_y\ (\frac{4\pi}{3})\ [0\ 0\ (L_r + L_{pin} + \frac{L_b}{2})]^T + ... \\
&\quad ... + R_y(0)\ [0\ (-L_{tool} - \frac{L_p}{2})\ 0]^T \\
[f_x\ f_y\ f_z]^T &= [e_x\ b_y\ e_z]^T
\end{aligned}$$

The matrix R_y is a standard rotational matrix.

$$R_y(\alpha) = \begin{pmatrix} \cos\alpha & 0 & \sin\alpha \\ 0 & 1 & 0 \\ -\sin\alpha & 0 & \cos\alpha \end{pmatrix} \quad (1)$$

The vectors pointing from the actuator positions to the points A, B, C, D, E, F on the platform are given below.

$$\begin{aligned}
\mathbf{A} &= [A_x\ A_y\ A_z]^T \\
\mathbf{B} &= [B_x\ B_y\ B_z]^T \\
\mathbf{C} &= [C_x\ C_y\ C_z]^T \\
\mathbf{D} &= [D_x\ D_y\ D_z]^T \\
\mathbf{E} &= [E_x\ E_y\ E_z]^T \\
\mathbf{F} &= [F_x\ F_y\ F_z]^T \quad (2)
\end{aligned}$$

$A_x, A_y, A_z, B_x, B_y, B_z, \cdots, F_x, F_y, F_z$ are the X-, Y- and Z-components of the normalised vectors pointing from the actuator positions to the points on the robot's platform, see Fig.2.

According to the kinematics, the vectors from the actuators to the points on the platform are:

$$\begin{aligned}
\mathbf{A} &= [(a_x^* + a_z^{**} + dX_1)\ (a_y + dY_1)\ (a_z^* - a_x^{**} + dZ_1)]^T \\
\mathbf{B} &= [(b_x^* + b_z^{**} + dX_2)\ (b_y + dY_2)\ (b_z^* - b_x^{**} + dZ_2)]^T \\
\mathbf{C} &= [(c_x^* + c_z^{**} + dX_3)\ (c_y + dY_3)\ (c_z^* - c_x^{**} + dZ_3)]^T \\
\mathbf{D} &= [(d_x^* + d_z^{**} + dX_4)\ (d_y + dY_4)\ (d_z^* - d_x^{**} + dZ_4)]^T \\
\mathbf{E} &= [(e_x^* + e_z^{**} + dX_5)\ (e_y + dY_5)\ (e_z^* - e_x^{**} + dZ_5)]^T \\
\mathbf{F} &= [(f_x^* + f_z^{**} + dX_6)\ (f_y + dY_6)\ (f_z^* - f_x^{**} + dZ_6)]^T \quad (3)
\end{aligned}$$

where $^* = \cos\alpha$, $^{**} = \sin\alpha$, X, Y, Z are the **TCP** coordinates. $dX_i = X - T_{ix}$, $dY_i = Y - T_{iy}$, $dZ_i = Z - T_{iz}$, where T_{ix}, T_{iy}, T_{iz} are the coordinates of actuator i for the given **TCP** position. Note, that T_{iy}, T_{iz} are constants and depend on support frame design parameters only, but T_{ix} is a function of the angle α. $[a_x a_y a_z]$, $[b_x b_y b_z]$, $[c_x c_y c_z]$, $[d_x d_y d_z]$, $[e_x e_y e_z]$, $[f_x f_y f_z]$ are the coordinates of the points A, B, C, D, E, F in the **TCP** coordinate frame. The constraints for all arms in the left-handed configuration are:

$$X_i \le X \qquad 0^0 \le r_y \le 90^0 \quad (4)$$

while the constraints for the right-handed configuration are

$$X_i \ge X \qquad -90^0 \le r_y \le 0^0 \quad (5)$$

The $\cos\alpha$ and $\sin\alpha$ equations are given below:

$$\begin{aligned}
\cos\alpha &= \frac{T_{3z} - Z}{\sqrt{L_{3m}^2 - (Y + M_y - T_{3y})^2} + \sqrt{M_x^2 + M_z^2}} \quad (6) \\
\sin\alpha &= \sqrt{1 - \cos^2\alpha} \quad (7)
\end{aligned}$$

L_{3m} is the middle length of the triangular-mounted arm 3. M_x, M_y, M_z are coordinates of a vector from a mid-point M between the triangular link coordinates C and E on the platform to the actuator position $(T_{3x} T_{3y} T_{3z})$, see Fig. 2 and given below:

$$\begin{aligned}
M_x &= C_x + \frac{E_x - C_x}{2} \quad (8) \\
M_y &= E_y \quad (9) \\
M_z &= C_z + \frac{E_z - C_z}{2} \quad (10)
\end{aligned}$$

A prototype of the 3-DOF Gantry-Tau with a triangular-mounted link pair built at the University of Agder, Norway is shown in Fig. 6. The kinematic parameters of the prototype are given below.

$$\begin{aligned}
Y_{offs} = 0.125 \quad (11) \\
Z_{offs} = 0 \quad Q_1 = 0.5m \quad Q_2 = 1m \quad (12) \\
T_{1y} = -Q_1 \quad T_{1z} = Q_1 \quad T_{2y} = 0 \quad (13) \\
T_{2z} = Q_2 \quad T_{3y} = 0 \quad T_{3z} = 0 \quad (14) \\
T'_{1y} = T_{2y} + Y_{offs} \quad T'_{1z} = T_{2z} - Z_{offs} \quad (15) \\
T'_{2y} = T_{2y} - Y_{offs} \quad T'_{2z} = T_{2z} - Z_{offs} \quad (16) \\
T'_{3y} = T_{3y} + Y_{offs} \quad T'_{3z} = T_{3z} + Z_{offs} \quad (17) \\
T'_{4y} = T_{3y} - Y_{offs} \quad T'_{4z} = T_{3z} + Z_{offs} \quad (18) \\
T'_{5y} = T_{3y} \quad T'_{5z} = T_{3z} + Z_{offs} \quad (19) \\
T'_{6y} = T_{1y} + Z_{offs} \quad T'_{6z} = T_{1z} - Y_{offs} \quad (20)
\end{aligned}$$

where Y_{offs} and Z_{offs} are distances from the base plate to the universal joint in Y and Z axis, T_{iy} T_{iz} are arm actuator positions and T'_{iy} T'_{iz} are link actuator positions.

3 The Distance Between Two Segments

The algorithm to define the closest distance between two line segments is presented. The distance between two

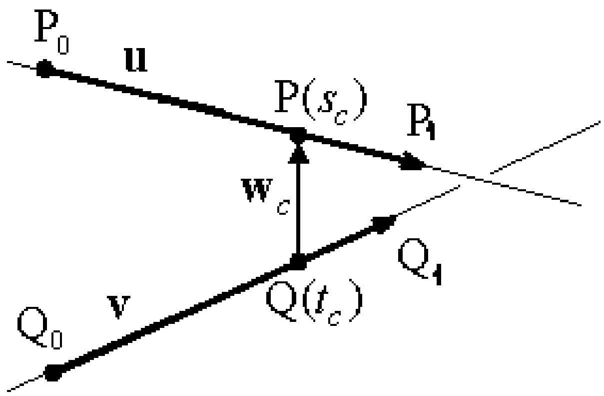

Figure 7: *Illustration of two lines and the minimum distance between them in 3D plane.*

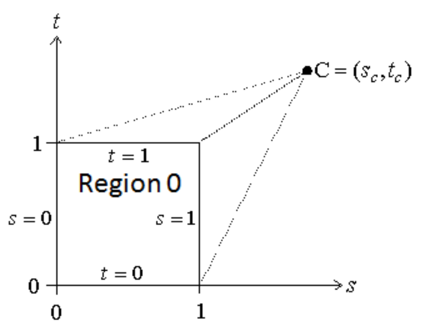

Figure 8: *Illustration of the minimum distance between lines in the st-plane.*

geometric objects (lines, segments of lines, rays, surfaces etc.) is defined as the minimum distance between two points on these objects. Two lines $P(s)$ and $Q(t)$ are shown in Fig.7 and parametric equations are given below.

$$P(s) = P_0 + s(P_1 - P_0) = P_0 + s\mathbf{u} \tag{21}$$
$$Q(t) = Q_0 + t(Q_1 - Q_0) = Q_0 + t\mathbf{v} \tag{22}$$

where P_0 and Q_0 are start points of line segments and P_1, Q_1 are end points, $\mathbf{u}$ and $\mathbf{v}$ are vectors pointed between start and end point of the line segments.

A vector between two points on line segments is given below.

$$\mathbf{w}(s,t) = P(s) - Q(t) \tag{23}$$

where $P(s)$ and $Q(t)$ are limited by line segment lower and upper boundaries. The distance between points $P(s_c)$ and $Q(t_c)$ on the line segments is a length of a vector $\mathbf{w}(s_c, t_c)$ and equals a minimum distance between two lines. According to the equations eqs.(21-23), the

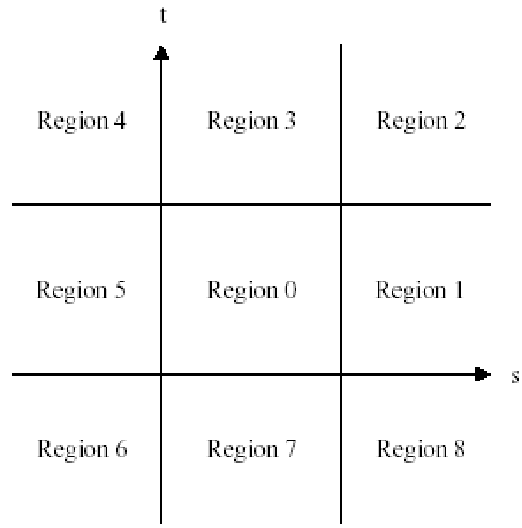

Figure 9: *Illustration of the st-plane divided by a unit square*

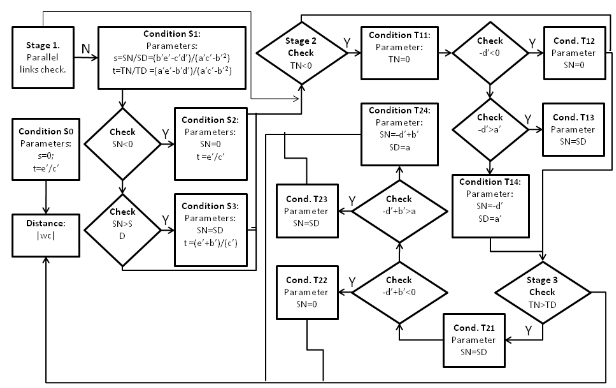

Figure 10: *Illustration of the boundaries search algorithm*

vector $\mathbf{w}_c$ is given below.

$$\begin{aligned} \mathbf{w}_c &= P(s_c) - Q(t_c) = P_0 + s_c\mathbf{u} - Q_0 - t_c\mathbf{v} = \\ &= \mathbf{w}_0 + s_c\mathbf{u} - t_c\mathbf{v} \end{aligned} \tag{24}$$

where the vector $\mathbf{w}_0$ is pointed between the line segment start points.

In addition, the vector $\mathbf{w}_c = \mathbf{w}(s_c, t_c)$ is also perpendicular to both unit vectors $\mathbf{u}$ and $\mathbf{v}$.

$$\mathbf{u} * \mathbf{w}_c = 0 \tag{25}$$
$$\mathbf{v} * \mathbf{w}_c = 0 \tag{26}$$

According to the eqs.(24-25), the vector scalar products $\mathbf{u} * \mathbf{w_c}$ and $\mathbf{v} * \mathbf{w_c}$ are given below.

$$(\mathbf{u} * \mathbf{u})s_c - (\mathbf{u} * \mathbf{v})t_c = -\mathbf{u} * \mathbf{w}_0 \tag{27}$$
$$(\mathbf{v} * \mathbf{u})s_c - (\mathbf{v} * \mathbf{v})t_c = -\mathbf{v} * \mathbf{w}_0 \tag{28}$$

The parameters s_c and t_c will be found from equations eqs.(27-28) and are given below.

$$s_c = \frac{b'e' - c'd'}{a'c' - b'^2} \qquad t_c = \frac{a'e' - b'd'}{a'c' - b'^2} \tag{29}$$

where a', b', c', d', e' are help variables

$$a' = \mathbf{u} * \mathbf{u} \qquad b' = \mathbf{u} * \mathbf{v} \qquad c' = \mathbf{v} * \mathbf{v}$$
$$d' = \mathbf{u} * \mathbf{w}_0 \qquad e' = \mathbf{v} * \mathbf{w}_0 \tag{30}$$

The denominator of the parameters s_c and t_c is greater or equals zero and given below.

$$a'c' - b'^2 = |\mathbf{u}|^2|\mathbf{v}|^2 - (|\mathbf{u}||\mathbf{v}|\cos\gamma)^2 = (|\mathbf{u}||\mathbf{v}|\sin\gamma)^2 \tag{31}$$

where γ is an angle between vectors $\mathbf{u}$ and $\mathbf{v}$. If the denominator is greater than zero, the lines are not parallel. If the denominator equals zero, the lines are parallel.

A distance between line segments and a distance between their extended lines may be different because the closest points between infinite line may be located outside of the segment range. The line segments between points $[P_0; P_1]$ and $[Q_0; Q_1]$ are given by eqs.(21-22), but two conditions are applied.

$$0 \le s \le 1 \qquad 0 \le t \le 1 \tag{32}$$

The closest distance between two line segments will be found in four stages.

Stage 1 : Check the segments if they are parallel. The parameters s_c and t_c for the parallel segments will be found from eq.(29), where one parameter equals zero. For example, $s_c = 0$, the solution of the equation system is given below.

$$s_c = 0 \quad \Rightarrow \quad s_c = \frac{b'e' - c'd'}{a'c' - b'^2} = 0 \quad \Rightarrow$$
$$\Rightarrow \quad b'e' - c'd' = 0 \quad \Rightarrow \quad b'e' = c'd' \quad \Rightarrow$$
$$\Rightarrow \quad e' = \frac{c'd'}{b'} \quad \Rightarrow \quad t_c = \frac{a'e' - b'd'}{a'c' - b'^2} \quad \Rightarrow$$
$$\Rightarrow \quad t_c = \frac{\frac{a'c'd'}{b'} - b'd'}{a'c' - b'^2} \quad \Rightarrow \quad t_c = \frac{a'c'd - b'^2 d'}{b'(a'c' - b'^2)} \quad \Rightarrow$$
$$\Rightarrow \quad t_c = \frac{d(a'c' - b'^2)}{b'(a'c' - b'^2)} \quad \Rightarrow \quad t_c = \frac{d'}{b'} = \frac{e'}{c'}$$

The parameters are $s_c = 0$ and $t_c = \frac{e'}{c'} = \frac{d'}{b'}$, if segments are parallel and stage 3 is applied to check the vertexes of the lines.

Stage 2 : Calculate the parameters s_c and t_c for the infinite lines as given in eq.(29). If the closest points are located inside of the segment ranges, no additional calculations are necessary. If the points are located outside of the segment ranges, new points will be found to define the length of the vector $\mathbf{w}_c$ as a minimum distance for the given segments and the third stage is applied.

Stage 3 : The boundary search method is used in this stage. A minimisation of the vector $\mathbf{w}$ is the same as a minimisation of $\mathbf{w}^2$.

$$\mathbf{w}^2 = (\mathbf{w}_0 + s\mathbf{u} - t\mathbf{v})(\mathbf{w}_0 + s\mathbf{u} - t\mathbf{v})$$

where $\mathbf{w}^2$ is a parabolic function of s and t, and a parabola will be defined in the st plane, where the minimum of the parabolic function is located at the point $C(s_c, t_c)$.

In Fig.8 the minimum of the parabolic function $C(s_c, t_c)$ and the unit square $Region_0$ are shown. The minimum $C(s_c, t_c)$ is located outside of the region $Region_0$, because the closest points between two line segments are located outside of the segment ranges. In this stage the "visible" boundaries for the point $C(s_c, t_c)$ will be found.

In Fig.8 four boundaries of the unit square $Region_0$ are given by $s = 0$, $s = 1$, $t = 0$, and $t = 1$. The point $C(s_c, t_c)$ is located in $Region_2$ in Fig.9. The boundary $s = 0$ is "visible" for the point $C(s_c, t_c)$ if $s_c < 0$. The boundary $s = 1$ is "visible" for the point $C(s_c, t_c)$ if $s_c > 1$. The boundary $t = 0$ is "visible" for the point $C(s_c, t_c)$ if $t_c < 0$. The boundary $t = 1$ is "visible" for the point $C(s_c, t_c)$ if $t_c > 1$. Up to two boundaries are "visible" for the point $C(s_c, t_c)$ if the point is located inside of diagonal regions $Region_2, Region_4, Region_6, region_8$ and one boundary if the point is located inside of $Region_1, Region_3, Region_5, Region_7$

In addition, a position of the minimum is found for each boundary. For example, the boundary is $s = 0$, $\mathbf{w}_c^2 = (\mathbf{w}_0 + 0\mathbf{u} - t_c\mathbf{v})^2 = (\mathbf{w}_0 - t_c\mathbf{v})^2$. The minimum of $\mathbf{w}_c^2$ is found from derivation.

$$0 = \frac{d}{dt}\mathbf{w}_c^2 = -2\mathbf{v}(\mathbf{w}_0 - t_c\mathbf{v})$$
$$t_c = \frac{\mathbf{v} * \mathbf{w}_0}{\mathbf{v} * \mathbf{v}} = \frac{e'}{c'} \tag{33}$$

The minimum is located at the point $(0; t_c)$ if t_c is inside of the range $0 \le t_c \le 1$. The minimum is located at the limits of the boundary t_c if t_c is outside of the range $0 \le t_c \le 1$ and two possible locations of the minimum are $(0; 0)$ or $(0; 1)$. Other three boundaries will be found in the similar manner.

However, two boundaries are "visible" for the minimum $C(s_c; t_c)$ in regions $2, 4, 6, 8$. Both boundaries will be taken into account and five possible solutions will be checked (two solutions for each boundary and one solution at the common point). In this stage the computational time will be reduced by the use of both boundaries at one time. The diagram of the boundary search method is shown in Fig.10.

Stage 4. Calculate the closest distance between two points as a length of the vector $\mathbf{w}_c$ from eq.(24).

4 Collisions analysis

This section presents new results compared to previous papers about the Gantry-Tau machine. The purpose of this work is to find a new method to quickly check for internal link collisions. A collision is deemed to have occurred if the minimum distance between two links in a given orientation is less than the diameter of the links. The conditions $S_0 - T_{24}$ for fifteen pairs of the links are given without identification and explanation how they are relevant because of limited space. The conditions were tested with different arm lengths and parameters Q_1 and Q_2. Full conditional equations and the explanations are given in Tyapin (2008).

Pairs $C - D$ and $A - B$ are parallel. The condition S_0 (see Fig.10) is used to define the minimum distance between the links. Additional check of the segment vertexes gave the negative result and conditions $T_{11} - T_{24}$ (see Fig.10) are not applied for the Gantry-Tau parallel links. The coordinates of the minimum $C(s_c, t_c)$ are $s_c = 0$ and $t_c = \frac{e'}{c'}$ and a vector $\mathbf{w_c}$ is given below.

$$\mathbf{w_c} \quad = \quad \mathbf{w_0} - \frac{e'}{c'}\mathbf{v} \tag{34}$$

According to the section 2 and eq.(34), the minimum distance between links $Dis = |\mathbf{w_c}|$ is given as follow.

$$Dis_{AB} = \frac{2T'_{iy}}{L_i}\sqrt{L_i^2 - (i_y + Y - T'_{ky})^2} \tag{35}$$

where T'_{iy} is the actuator position of the links $\mathbf{D}$ or $\mathbf{B}$, T'_{ky} is the actuator position of the links $\mathbf{A}$ or $\mathbf{C}$, i_y is Y-coordinate of the points D or B, L_i is a length of the vectors $\mathbf{D}$ or $\mathbf{B}$. All these parameters are constants and Y is a current Y-coordinate of the TCP.

The minimum distance equation for the links $\mathbf{C} - \mathbf{D}$ or $\mathbf{A} - \mathbf{B}$ depends on Y-position of the TCP and the distance will be found once for fixed Z and unconstraint Y- coordinate of the TCP.

Pairs $E - A$ and $E - B$ are not parallel, and the condition S_3 is applied for any YZ-position of the TCP, see Fig.10. The coordinates of the minimum $C(s_c, t_c)$ are $s_c = 1$ and $t_c = \frac{e'+b'}{c'}$ A vector $\mathbf{w_c}$ for the pair $E - A$ is given below.

$$\mathbf{w_c} \quad = \quad \mathbf{E_A} - \frac{e'+b'}{c'}\mathbf{v} \tag{36}$$

where a vector $\mathbf{E_A}$ is pointed from the actuator position of the link $\mathbf{A}$ to the point E on the platform.

A parameter t_c will be simplified and an equation is given below.

$$\begin{aligned} t_c \quad = \quad & \frac{1}{L_A^2}(dX^2 + dZ^2 + dY^2 + e_x a_x + a_z e_z + a_y e_y + ... \\ & ... + dY(e_y) + cos\alpha(a_x dX + e_x dX + a_z dZ + e_z dZ) + ... \\ & ... + dY(a_y) + sin\alpha(a_z dX + e_z dX - a_x dZ - e_x dZ)) \end{aligned} \tag{37}$$

Note that a vector $\mathbf{w_c}$ is the same for a pair $E - B$, but instead of $(a_x\ a_y\ a_z)$ the coordinates of the point B are used.

According to the section 2 and eq.(36), the minimum distance between links $Dis = |\mathbf{w_c}|$ is given as follow.

$$Dis_{EA} = \sqrt{|\mathbf{E_A} - t_c \mathbf{A}} \tag{38}$$

The minimum distance equation for the links $\mathbf{E} - \mathbf{A}$ or $\mathbf{E} - \mathbf{B}$ depends on Y and Z-position of the TCP. The distance will be found for each point of the workspace, but the constant coordinates of the points on the platform in TCP coordinate frame will be added into account.

Pairs $E - C$ and $E - D$ are not parallel, and the conditions S_2 and T_{14} (see Fig.10) are applied and depend on Y-position of the TCP. The coordinates of the minimum $C(s_c, t_c)$ are $s_c = 0$ and $t_c = \frac{e'}{c'}$ (condition S_2) and $s_c = \frac{-d'}{a'}$ and $t_c = 0$ (condition T_{14}).

The condition S_2 is used if the Y-coordinate of the vector $\mathbf{C}$ or $\mathbf{D}$ is negative. Since the Y coordinate is positive the condition T_{14} is applied. The Y coordinate is a control point (see section 3). According to the section 2 the minimum distance between links will be found as follows.

$$if \qquad (d_y + dY_4) < 0 \ or \ (c_y + dY_3) < 0 \tag{39}$$

$$1 \ : \ Dis_{EC} = \frac{T'_{ky}}{L_k}\sqrt{L_k^2 - (k_y + Y - T'_{ky})^2} \tag{40}$$

$$if \qquad (d_y + dY_4) \geq 0 \ or \ (c_y + dY_3) \geq 0 \tag{41}$$

$$2 \ : \ Dis_{EC} = \frac{T'_{iy}}{L_i}\sqrt{L_i^2 - (i_y + Y - T'_{iy})^2} \tag{42}$$

where i indicates the vector $\mathbf{E}$ and k indicates the vector $\mathbf{C}$ or $\mathbf{D}$. where $T'_{ky}, T'_{iy}, k_y, i_y, L_k, L_i$ are constants and Y is current Y-coordinate of the TCP. The minimum distance function for the links $\mathbf{E} - \mathbf{C}$ and $\mathbf{E} - \mathbf{D}$ only depends on y-position of the TCP.

Pairs $C - A$ and $C - B$ are not parallel and conditions S_3, T_{23} (see Fig.10) are applied. The coordinates of the minimum $C(s_c, t_c)$ are $s_c = 1$ and $t_c = \frac{e'+b'}{c'}$ (condition S_3) and $s_c = 1$ and $t_c = 1$ (condition T_{23}).

The distance equation for the pair $C - A$ is not the same as for $E - A$ but will be simplified in the similar way. The general equation for the condition S_3 is given as follows.

$$Dis_{S3} = \sqrt{(U_x - T'_{vx} - K_{17}(x,y,z)(V_x + T'_{vx}))^2 + ... \\ ... + (U_y - T'_{vy} - K_{17}(x,y,z)(V_y + T'_{vy}))^2 + ... \\ ... + (U_z - T'_{vz} - K_{17}(x,y,z)(V_z + T'_{vz}))^2}$$

where U_x, U_y, U_z are the coordinates of a first vector and equals coordinate of the point on the platform plus TCP position, V_x, V_y, V_z are the coordinates of a second vector and $K_{17}(x,y,z)$ is given below.

$$\begin{aligned} K_{17}(x,y,z) &= \frac{1}{L_V^2}((2U_x - T'_{vx} - T'_{ux})(V_x - T'_{vx}) + ... \\ ... &\quad +(2U_y - T'_{vy} - T'_{uy})(V_y - T'_{vy}) + ... \\ ... &\quad +(2U_z - T'_{vz} - T'_{uz})(V_z - T'_{vz})) \end{aligned} \tag{43}$$

In the next stage the kinematics will be used to simplify the equation 43. In addition, the control points will be found as given below.

$$s_N > s_D \;\Rightarrow\; b'(e'+b') > c'(a'+d') \tag{44}$$

$$e' + b' = K_{17}(x,y,z)L_V^2 \tag{45}$$

$$a' + d' = (U_x - T'_{ux})(U_x - T'_{vx}) + ... \\ ... + (U_y - T'_{uy})(U_y - T'_{vy}) + (U_z - T'_{uz})(U_z - T'_{vz}) \tag{46}$$

The inequality 44 is easy to be checked if all kinematic parameters are used instead of variables.

The general distance equation for the condition T_{23} is given below.

$$Dis_{T_{23}} = \sqrt{(u_x - v_x)^2 + (u_y - v_y)^2 + (u_z - v_z)^2} \tag{47}$$

where $u_x\ u_y\ u_z$ are coordinates of the first vector. Note that the coordinates are given in TCP frame. The solution T_{23} is a constant for any given TCP coordinates and depends on coordinates of the points on the platform.

In addition, the control points will be found as given below.

$$b' - a' - d- > 0 \tag{48}$$

$$(U_x + T'_{ux})(V_x - 2U_x + T'_{ux}) + ... \\ ... + (U_y + T'_{uy})(V_y - 2U_y + T'_{uy}) + ... \\ ... + (U_z + T'_{uz})(V_z - 2U_z + T'_{uz}) > 0 \tag{49}$$

The inequality will be solved if the kinematic parameters are added.

A pair $B-F$ is not parallel and conditions $S_1,\ T_{24}$ (see Fig.10) are applied. The coordinates of the minimum $C(s_c, t_c)$ are $s_c = \frac{b'e' - c'd'}{a'c' - b'b'}$ and $t_c = \frac{a'e' + b'd'}{a'c' - b'b'}$ (condition S_1) and $s_c = \frac{-d' + b'}{a'}$ and $t_c = 1$ (condition T_{24}).

The general distance equation for the condition S_1 is too long to be presented in this paper. The general distance equation for the condition T_{24} is given below.

$$Dis_{24} = \sqrt{(-V_x + T'_{ux} + K_{24}(x,y,z)(U_x - T'_{ux}))^2 + ... \\ ... + (-V_y + T'_{uy} + K_{24}(x,y,z)(U_y - T'_{uy}))^2 + ... \\ ... + (-V_z + T'_{uz} + K_{24}(x,y,z)(U_z - T'_{uz}))^2} \tag{50}$$

$$K_{24}(x,y,z) = \frac{(U_x - T'_{ux})(V_x - U_x)}{L_U^2} + ... \\ ... + \frac{(U_y - T'_{uy})(V_y - U_y) + (U_z - T'_{uz})(V_z - U_z)}{L_U^2} \tag{51}$$

where the kinematic parameters will be added into equation to simplify it.

In addition, the control points will be found as given below.

$$e' + b' - c > 0 \tag{52}$$

$$(V_x + T'_{vx})(U_x - V_x) + (V_y + T'_{vy})(U_y - V_y) + ... \\ ... + (V_z + T'_{vz})(U_z - V_z) > 0 \tag{53}$$

The inequality will be solved if the kinematic parameters are added.

Last six pairs are not presented in this paper because of limited space. However, the conditions are $S_3,\ T_{23},\ T_{24}$ for pairs $E-F$ and $A-D$ and $T_{24},\ T_{23}$ for pairs $C-F$, $A-F$ and $B-D$. In addition, the conditions $S_1,\ S_3$ are applied for a pair $F-D$, see Fig.10 and section 2

5 Optimisation problem

An optimal design for the Gantry-Tau (and other PKMs) is difficult to find manually. In this section an optimisation scheme based on the geometric descriptions of the workspace, unreachable area and a functional dependency of the collisions calculation is presented. The optimisation problem is expressed as

$$\begin{aligned} &\max V_R(Q_1, Q_2, L_1, L_2, L_3) \\ &\text{subject to} \\ &V_U(Q_1, Q_2, L_1, L_2, L_3) \\ &L_C^* > 0.05 \quad Q_1 > 0 \quad Q_2 > 0 \\ &L_A > 0 \quad L_B > 0 \quad L_C > 0 \\ &L_D > 0 \quad L_E > 0 \quad L_F > 0 \end{aligned}$$

where V_R is the total workspace volume, L_C^* is the minimum distance between two robot's links. V_U is the unreachable area volume in the middle of the workspace caused by long arms and short actuators. These area exist even if the robot can be reconfigured between the left-hand and right-hand inverse kinematic solutions and can significantly reduce the workspace of the Gantry-Tau. The unreachable area was presented before in Tyapin, Hovland and Brogårdh (2007a). The collisions are detected if the distance is less or equals 0.05 m (the diameter of the link). $L_A - L_F$ are the link lengths. Q_1, Q_2 are the support frame parameters.

The total workspace volume V_R as a function of the two support frame design parameters Q_1, Q_2 and the individual link lengths $L_A - L_F$ is maximised while the minimum distance between the links is greater than 0.05 m (no collisions are detected) and and the unreachable area volume equal to zero. Since the track lengths are fixed and equal to $2.0m$, the unreachable area volume will appear if the link lengths become too large. Hence, the unreachable volume is effectively an upper bound on the total achievable workspace when fixed length actuators are used. Without including the unreachable area volume into the workspace optimisation, it would not be possible to simultaneously optimise both the support frame parameters Q_1, Q_2 and the link lengths $L_A - L_F$ as these would all go to infinity. The optimisation results are presented in section 6.

6 Results

The final optimisation design parameters of the Gantry-Tau were found using the *lsqnonlin* function in Matlab. The optimisation results are given below:

$$\begin{aligned}
&Q_1 = 0.5155 \quad Q_2 = 1.0212 \quad V_R = 3.6999 \\
&L_C^* = 0.0901 \quad V_U = 0 \\
&L_F = 0.9482 \quad L_A = 0.9514 \quad L_E = 0.9467 \\
&L_C = 0.9467 \quad L_B = 0.9514 \quad L_D = 0.9467
\end{aligned} \tag{54}$$

These results would have been difficult to obtain by a manual design, as all the link lengths are different and Q_2 is different from $2Q_1$ which has been a typical manual design choice of the Gantry-Tau in the past. The required installation space of the Gantry-Tau equals $2Q_1Q_2 = 1.05m^3$ for the optimised design. Hence, the total workspace to installation space ratio for the optimised design is $V_{installation} = 3.5228\ m^3$ which is large compared to most other PKMs which typically have a ratio of less than one.

7 Conclusions

A new design optimisation of 3-axis version of the Gantry-Tau parallel kinematic manipulator has been presented in this paper. In addition, the geometric approach to define the workspace and the functional dependency of the cross-sectional workspace area on the robot's X coordinate is used to calculate the total workspace volume (see Tyapin, Hovland and Brogårdh (2007)) and the unreachable area volume (see Tyapin, Hovland and Brogårdh (2007a)) and the functional dependency to detect the collisions between links have been developed. The collision detection approach is an extension of the method in Murray, Hovland and Brogård (2006). The method is based on a functional dependency of the elements of the static matrix $\mathbf{H}$ and the Cartesian position vector $\mathbf{X}$. In addition, the relations between vectors were taken into account.

The Gantry-Tau is a part of HEXAPOD family parallel kinematic manipulator and the use of the conditional equations to define the collisions free workspace is applicable for the other machines from the family (H4, Orthoglide, Delta, etc.), but an additional analysis of the links properties is necessary.

Method	**Time**
Method in Murray (2006)	15
Method in Teller (2008)	11
Functional Dependency	1

Table 1: Collisions detection computation time for three different methods.

Table 1 shows the computational requirements for the three different approaches on the triangular version of the 3-DOF Gantry-Tau PKM. The method based on the functional dependency is 15 times faster than the method presented in Murray, Hovland and Brogård (2006). The computational time has been normalized to 1 for the third approach.The drawbacks of the method presented in this paper are conditional control points. For example, the conditions S_3 and T_{24} (see Fig.10) are used to define the closest distance between two line segments, where the condition S_3 is applicable while the Y coordinates of the segment end points are positive. The additional calculation is used to find the Y coordinates, when the condition S_3 changes to T_{24}.

The collision analysis shows that the design of the manipulated platform is crucial to avoid link collisions and different platform design could be needed if the robot will be used in both left hand and right hand configurations. An optimisation routine for the platform design would be a challenging future research topic. In addition, the algorithms developed in this paper allow for a fast workspace analysis and customisation of each individual Gantry-Tau machine design, depending on the work object requirements. For a complete automation design, potential collisions with the work objects should also be considered.

The results in this paper show that it is possible to optimise the kinematic design of the Gantry-Tau PKM to achieve no collisions between links while maximising the reachable workspace and keeping unreachable area equals zero.

Future extensions of the work presented in this paper will introduce performance criteria such as the Cartesian stiffness, singularities and first resonance frequency into the design optimisation.

8 Acknowledgement

I would like to thank Torgny Brogårdh of ABB, Sweden and Geir Hovland of University of Agder, Norway for their contributions to this work.

References

T. Brogårdh, S. Hanssen and G. Hovland, Application-oriented development of parallel kinematic manipulators with large workspace, *Proc. 2nd International Colloquium of the Collaborative Research Center 562:Robotic Systems for Handling and Assembly*, Braunschweig, Germany, May 2005, pp. 153–170.

S. Johannesson, V. Berbyuk, and T. Brogårdh, A new three degrees of freedom parallel manipulator, *Proc. 4th Chemnitz Parallel Kinematics Seminar*, Chemnitz, Germany, Apr. 20–21, 2004, pp. 731–734.

M. Murray, G. Hovland and T. Brogårdh, Collision-Free Workspace Design of the 5-Axis Gantry-Tau Parallel Kinematic Machine, *Proc. of the 2006 IEEE/RSJ Intl. Conference on Intelligent Robots and Systems,*, Beijing, October 2006.

I. Tyapin, G. Hovland and T. Brogårdh, A Fully Geometric Approach for the Workspace Area of the Gantry-Tau Parallel Kinematic Manipulator, *Proc. of the 13th IASTED International Conference on Robotics and Applications*, Wurzburg, Germany, August, 29-31, 2007.

I. Williams, G. Hovland and T. Brogårdh, Kinematic Error Calibration of the Gantry-Tau Parallel Manipulator, *Proc. of the IEEE Intlernational Conference on Robotics and Automation*, Orlando, May 2006.

D. Teller, Distance Between Two Line Segments in 3D, *Geometric tools, LLC*, http://www.geometrictools.com, 1998-2008.

D. H. Eberly, 3D Game Engine Design, *Morgan Kaufmann*, pp. 561, 2001.

G. Hovland, M. Choux, M. Murray, I. Tyapin and T. Brogårdh, The Gantry-Tau Summary of Latest Development at ABB, University of Agder and University of Queensland, *Proc. of the 3rd Intl. Colloquium: Robotic Systems for Handling and Assembly, the Collaborative Research Centre SFB 562*, Braunschweig, Germany, April 2008.

T. Brogårdh, PKM research - important issues, as seen from a product development perspective at ABB Robotics, *Proc. of the Workshop on Fundamental Issues and Future Research Directions for Parallel Mechanisms and Manipulators*, Quebec, Canada, Oct. 2002.

I. A. Bonev, J. Ryu, A Geometrical Method for Computing the Constant-Orientation Workspace of 6-PRRS Parallel Manipulator, *Mechanism and Machine Theory*, Vol. 36, No. 1, pp. 1, 2001.

X.-J. Liu, J.-S. Wang, F. Gao, On the Optimum Design of Planar 3-DOF Parallel Manipulators with Respect to the Workspace, *Proc. of the International Conference on Robotics and Automation*, San Francisco, April, 2000.

D. J. Kim, W. K. Chung and Y. Youm, Geometrical Approach for the Workspace of 6-DOF Parallel Manipulators, *Proc. of the IEEE International Conference on Robotics and Automation*, Albuquerque, New Mexico, April, 1997.

J.-P. Merlet, *Parallel Robots*, Kluwer Academic Publisher, Solid Mechanics and its Applications, Dordrecht, Boston, Vol. 74, 2000,

D. Chablat and P. Wenger, Architecture Optimisation of a 3-DOF parallel mechanism for machining applications, the Orthoglide, *ITEE Transactions on Robotics and Automation*, Vol. 19, No. 3, pp. 403-410, 2003.

J. C. Hudgens and T. Arai, Planning Link-Interference-Free Trajectories for a Parallel Link Manipulator, *Proc. of the IEEE Intl. Conf. on Industrial Electronics, Control and Instrumentation*, Hawaii, November, pp. 1506-1511, 1993.

B. Monsarrat and C. Gosselin, Workspace Analysis and Optimal Design of a 3-Leg 6-DOF parallel Platform Mechanism, *Transactions on Robotics and Automat.*, pp. 954-966, Vol. 19, 2003(6).

I. Tyapin, Design Optimisation of Parallel Kinematic Machines, *Ph.D Thesis*, The University of Queensland, November, 2008.

I. Tyapin, G. Hovland and T. Brogårdh, Workspace Optimisation of Reconfigurable Parallel Kinematic Manipulator, *Proc. of the IEEE/ASME International Conference on Advanced Intelligent Mechatronics*, Zurich, Switzerland, Sept. 4-7, 2007.